Airborne Radar Observations of the Flight Behavior of Small Insects in the Atmospheric Convective Boundary Layer

BART GEERTS[1] AND QUN MIAO

Department of Atmospheric Science, University of Wyoming, Laramie, WY 82071

Environ. Entomol. 34(2): 361–377 (2005)

ABSTRACT The vertical flight behavior of insects in the convective boundary layer (CBL) is examined by means of profiling airborne Doppler radar data collected in the central Great Plains in late spring. On fair-weather days, the CBL grows from the ground up in morning hours and matures at a depth of 1,000–1,500 m shortly after midday. It is well mixed by thermals bubbling up from near the surface. Nevertheless the CBL is dominated, over its entire depth, by well-defined regions of high insect concentrations, here referred to as insect plumes. This is inferred from radar, whose echoes in the CBL are largely caused by microinsects (<10 mm diameter). This study focuses on the vertical motion of the radar scatterers relative to the vertical air motion, in natural conditions. It is shown that insect plumes tend to be collocated with updrafts in the CBL and that microinsects tend to fall or fly down against the updrafts at an average speed of 0.5 ± 0.2 m/s. This estimate is based on a comparison of the close-range radar velocities, some 100 m above and below the aircraft, with the vertical air velocity measured at flight level. We hypothesize that the gregarious behavior of small insects in the CBL is explained by their tendency to oppose updrafts at a rate that is surprisingly proportional to the updraft strength. This finding is also strong evidence for the biotic nature of the echo plumes. This hypothesis is tested elsewhere by means of a simple numerical simulation.

KEY WORDS microinsect flight, insect plumes, convection, atmospheric boundary layer, Doppler radar

THE CONVECTIVE BOUNDARY LAYER (CBL) is the atmospheric layer within which buoyant plumes of air (thermals) transfer heat from the surface of the earth. It is marked by turbulent air motion and is capped by a stable layer in which the airflow is much smoother (e.g., Stull 1988). The turbulence is caused by convection: buoyant thermals tend to rise at speeds up to ≈5 m/s and are surrounded by compensating downdrafts. This turbulence explains why passive tracers, such as dust or water vapor, are rather well-mixed in the CBL. The turbulence presents an obvious flight challenge, both to weakly and strongly flying insects. The CBL is best developed over land, on clear, calm days during late spring and early summer, when the net radiation at the surface is largest. The mature CBL is typically 1 km deep, although this depth varies considerably (e.g., Stull 1988). It grows in depth during the morning and collapses near sunset in response to diurnally changing surface heat fluxes.

The wavelengths used by conventional weather radars range between 3 and 10 cm. At these wavelengths, precipitation particles (such as rain or snow) effectively scatter the radiation, producing a strong radar "echo." However, these radars often see echoes in the clear air, entirely free of precipitation (Atlas 1959; a good review can be found in Gossard 1990). The clear-air scatterers are mostly biotic (e.g., Russell and Wilson 1997), and thus, the entomology community has embraced the use of weather radar to study insect flight behavior, following the pioneering work of Schaefer (1976) in Africa. A new generation of "entomological" radars resulted, designed specifically to study airborne insects. These radars usually operate in the X-band (3 cm wavelength), both in scanning and vertically profiling modes (Dean and Drake 2002). Much experimental research on insect flight behavior has been done with such radars. In fact, even weather radar networks that operate continuously, such as the scanning S-band (10 cm) Weather Surveillance Radar v. 1988-D (WSR-88D) network in the United States, are used increasingly to routinely monitor insect densities and migration. Most of the entomological work with radar has focused on macroinsects, especially to study the migration and dispersion patterns of agricultural pests such as locusts (Schaefer 1976, Reynolds 1988). (The radar entomology literature counts over 200 papers. See http://www.ph.adfa.edu.au/a-drake/trews/ for other references.)

There is some evidence in the literature that the insect scatterers in the CBL are mostly microinsects (long axis < 10 mm) (e.g., Vaughn 1985, Russell and Wilson 1997). These insects have been referred to as

[1] Corresponding author, e-mail: geerts@uwyo.edu.

0046-225X/05/0361–0377$04.00/0

aerial plankton (Drake and Farrow 1989) because they are weakly flying. Their deliberate or inadvertent movement from their foraging range into the CBL will result in dispersal and migration into a new territory, but this migration is passive, i.e., wind-driven. Russell and Wilson (1997), examining regions of enhanced reflectivity in the CBL, suggest that birds and other aerial predators contribute <2% of the radar return power. The remaining 98% are insects, including macroinsects, which tend to be strongly flying. Daytime concentrations of macroinsects in the CBL have been detected by radar (e.g., Schaefer 1976, Reid et al. 1979, Reynolds 1988, Achtemeier 1991). These include day-flying locusts and grasshoppers, dragonflies, monarch butterflies, and other types of butterflies. Most strongly flying insects, however, migrate at night when the lower atmosphere is stably stratified (Richter et al. 1973, Drake 1985), because during the day, the strong vertical drafts in the CBL make migration difficult. It is unclear to us what the relative contribution of micro- and macroinsects to the measured reflectivity (and Doppler velocity) typically is in the daytime CBL in late spring over the central Great Plains. The literature also is not clear on this. We suspect that while microinsects generally dominate, the ratio of micro- to macroinsects probably is highly variable in the CBL, locally, regionally, and temporally.

If microinsects dominate the CBL echoes for conventional weather or entomological radars, this is a fortiori true for shorter-wavelength radars, such as the 3-mm "cloud" radar (W-band) used in this study. That is because the scattering cross section of microinsects, relative to that of macroinsects, is much larger at W-band than at S-band. Clothiaux et al. (2000) used a sensitive, zenith-pointing cloud radar to show that, at 1 km above ground level (AGL), ≈90% of the radar data are dominated by insect echoes in the warm season at a site in Oklahoma (see their Fig. 12).

Microinsect distribution in the CBL is far from uniform (Konrad 1970, Vaughn 1985, Drake and Farrow 1988, Riley 1999). The existence of "insect plumes" is remarkable given that the convective motions effectively mix the CBL, so any conserved quantity, such as the concentration of pollen, tends to become nearly uniformly distributed after some time (Weckwerth et al. 1996). The mixing time scale can be estimated, assuming a characteristic CBL depth of 1,000 m and a characteristic vertical velocity profile that peaks at 2 m/s in the central CBL. The time required to travel up and down once through 90% of the depth of the CBL is ≈25 min. Numerical simulations (e.g., Mason 1989) and observations of cellular patterns on scanning weather and entomological radars (Markowski 2004, A. Drake, personal communication) confirm that the life cycle of CBL thermals typically is on the order of 1 h. Thus, the mixing time scale is much shorter than the daily cycle, which supports a CBL for ~6–9 h.

The radar-based study of Schaefer (1976) was the first to show that atmospheric convergence zones can congregate insects in the CBL. Hardy and Ottersten (1969) showed a radar reflectivity map with polygonal cells with a diameter of ≈5 km and a maximum height of ≈2 km. Such honeycomb patterns typically occurs under light wind, little wind shear, and strong surface heat fluxes (LeMone 1973). Reid et al. (1979) documented a banded echo structure, which may be caused by helical roll circulations in a sheared CBL. Less well-defined patterns are observed more commonly, intermediate between bands and polygonal cells (Hardy and Ottersten 1969, Konrad 1970).

Aside from these regular patterns across the radar domain, a narrow, singular line of high insect concentration may be observed. Such "fine-lines" may be hundreds of kilometers long (Russell and Wilson 1997). In fact, the operational WSR-88D radars use a special "clear-air" volume coverage pattern specifically to monitor insect dispersal in the CBL during the warm season. The reason that forecasters monitor fine-lines is that they turn out to be the most likely area of thunderstorm initiation (e.g., Wilson and Schreiber 1986). The reason for this seems to be sustained confluence of air from opposite sides of the line, leading to convergence and a concentration of not only insects, but also heat and moisture sufficient to trigger deep convection (Wilson et al. 1994).

It is now generally accepted that fine-lines can be detected by radar because insects congregate in them (Schaefer 1976, Greenbank et al. 1980, Drake 1982, Pedgley et al. 1982, Drake and Farrow 1989). The same applies to the cellular or banded echo structures mentioned above: microinsects concentrate in the updraft regions of these periodic CBL airflow patterns. In fact, reflectivity differences suggest that the concentrations are one to three orders of magnitude higher in the fine-lines compared with the background. This is a nice example of how insect flight behavior has come to reveal atmospheric circulations and assist in weather prediction.

The question then arises as to what flight strategy microinsects use that results in the highly heterogenous insect concentration in the CBL. This is especially remarkable because CBL turbulence tends to homogenize concentrations of passive tracers. It should be emphasized that the question regards microinsect distribution in the daytime CBL. Much work has been done to describe the movement and concentration of strongly flying macroinsects by means of radar data and to interpret the observations in terms of their flight behavior (e.g., Schaefer 1976, Greenbank et al. 1980). It seems from the literature that the fundamental question of how weakly flying microinsects concentrate in the CBL remains unanswered. This is the key question addressed in this paper.

Insect motion has been studied extensively by means of ground-based Doppler radars (e.g., Pedgley et al. 1982, Vaughn 1985, Reynolds 1988, Wilson et al. 1994, Dean and Drake 2002). One recurring challenge has been to discriminate air motion from insect motion relative to the air. In this study, an airborne Doppler radar is used on an aircraft equipped with a gust probe to measure winds in three dimensions. Winds are measured in close proximity to the radar-inferred velocities. Thus, after correction for aircraft motion, the

insect motion can be isolated from air motion, at least approximately.

The aircraft, the Wyoming King Air, was flown on several clear days in May and June of 2002 over mostly cultivated land in the central Great Plains of North America. It was equipped with an array of instruments for atmospheric research, including temperature and humidity sensors, but neither insect morphology nor concentration were sampled. Therefore, no direct evidence was collected about the scatterers, although on several occasions, the aircraft windshield was largely covered with insect debris after some 3 h of flight in the CBL (Admittedly, this debris was mostly derived from macroinsects). If questions remain about the scatterers, this paper should provide indirect but convincing evidence of their biotic nature.

Because we aimed to address the question about what keeps the weakly flying microinsects aloft in a very turbulent CBL, we focused on a comparison between the vertical air motion and the radar-inferred vertical velocity (which includes both insect and air motions). The aircraft carried both nadir and zenith radar antennas. The nearest-gate Doppler velocities below and above the aircraft can be compared directly to the aircraft gust probe measurements, after careful correction for aircraft motion. The nearest gates are ≈100 m above and below the aircraft, so the vertical air motion at the flight level of the insects is not quite known. However, the resulting estimates of insect vertical motion in the free atmosphere, as presented herein, are believed to be unprecedented.

The combined radar and aircraft measurements are the focus of this study. However, first the structure and vertical velocity characteristics of insect plumes in the CBL are described. The observed discrepancy between gust-probe and radar vertical velocities leads to a hypothesis of insect response to ambient vertical air motion. This hypothesis is tested by means of a simple numerical model in Geerts and Miao (2005).

Materials and Methods

About 30 h of combined radar and in situ aircraft data were collected in the mature CBL in May to June 2002. In most cases, the sky was clear, and the wind was relatively light, and no weather disturbances such as thunderstorms or fronts were present. Flight levels varied from 60 m AGL to a few hundred meters above the CBL, and aircraft-based soundings from the ground to ≈500 m above the CBL top were collected regularly. The data shown here come mainly from flights along three fixed tracks, in length ranging between 45 and 60 km, each of them flown 12–18 times in either direction (Fig. 1). One was oriented north-south in the Oklahoma Panhandle (the "western track") over irrigated farmland and uncultivated prairie. This land is very flat except for the Beaver Creek valley, which is ≈ 60 m below the plain. A second track (the "central track") was east-west oriented in southcentral Kansas, covering equally flat terrain of mostly green pastures. A third track, the "eastern track," ≈100 km east of the second track,

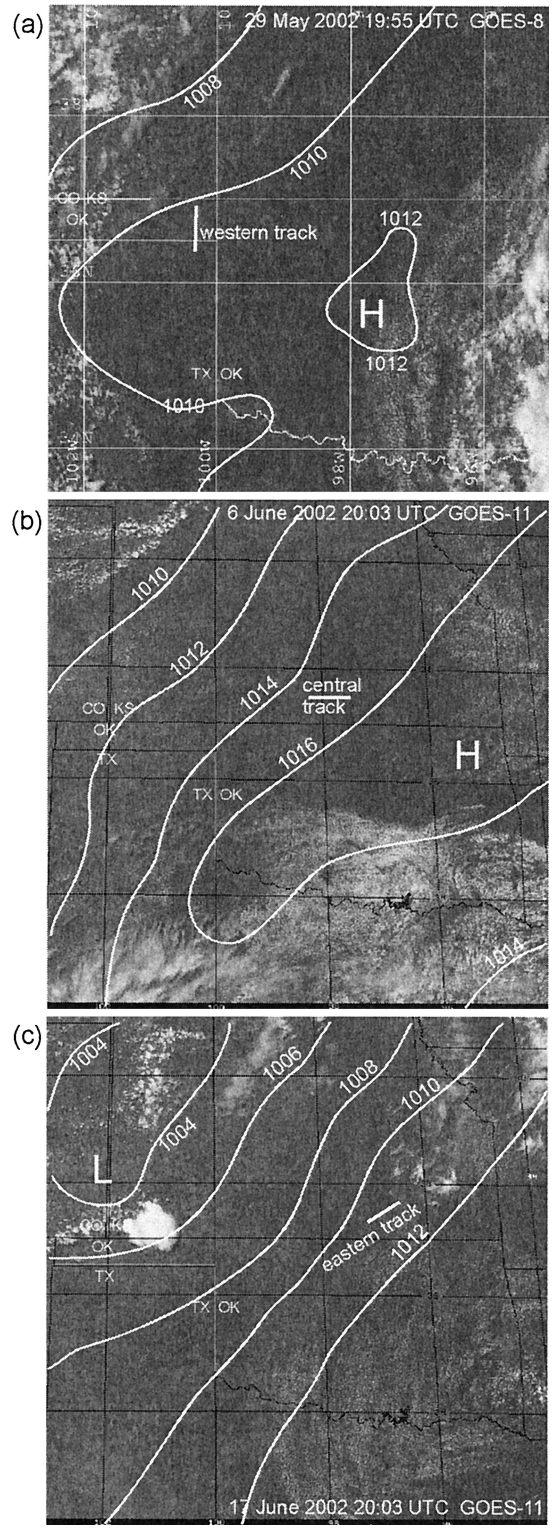

Fig. 1. Visible satellite images of the central Great Plains near 20 UTC (15 CDT) on (a) 29 May, (b) 6 June, and (c) 17 June 2002. Also shown are the location of the flight track and the 20 UTC sea level pressure analysis.

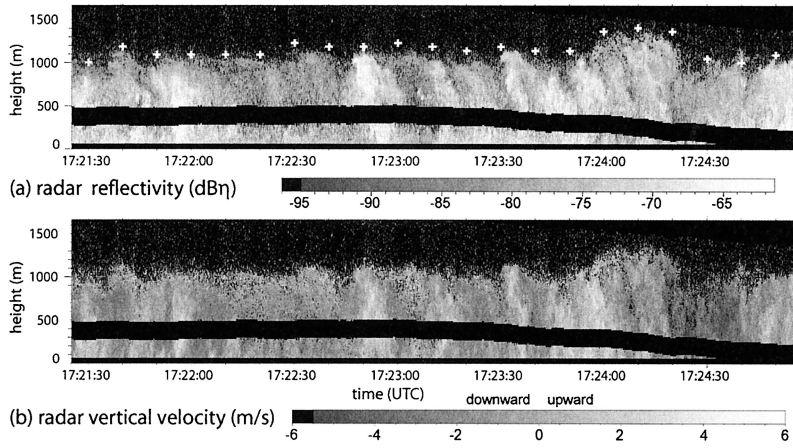

Fig. 2. (a) Radar reflectivity and (b) WCR vertical velocity for a sample transect of the CBL on 29 May 2002 on the western flight track (Fig. 1). The vertical axis is height AGL; the horizontal axis is time (1 min of flight corresponds with a distance of ≈ 5 km). White stars in the top panel indicate $z_{i\ WCR}$, determined based on the reflectivity gradient. The black belt is a 225-m-deep "blind zone." The aspect ratio of both images is ≈2:1.

contained slightly undulating land of pastures and crops and a topographic ridge at the east end.

The radar used here, the Wyoming Cloud Radar (WCR), is a 3-mm radar normally used for cloud studies (Pazmany et al. 1994). The WCR has two simultaneously operating antennas looking up and down from the aircraft. The range resolution is 15–30 m, and the first reliable radar data are obtained at a range of 120 (nadir) and 105 m (zenith) from the aircraft, so there is an ≈225-m blind zone centered at flight level. The aircraft is equipped with a gust probe; therefore, high-frequency three-dimensional wind measurements are available in the middle of this blind zone.

Results

Plumes of Microinsects in the CBL

Radar Reflectivity and Insect Concentration. The presence of insect echo plumes in the clear CBL, at least in the warm season or in the tropics, has been shown (e.g., Konrad 1970, Schaefer 1976, Reid et al. 1979, Gossard 1990). These studies were all based on centimeter-wave radars. At those wavelengths, clear-air echoes, sometimes referred to as angel echoes (Atlas 1959), can be caused by inhomogeneities in the refractive index of the air (Bragg scattering). The question of whether angel echoes are caused by particle (insect) scattering or Bragg scattering has been controversial for years (Hardy et al. 1966, Atlas et al. 1970, Konrad 1970). However Bragg scattering, caused by refractive index turbulence at a scale of ≈1.6 mm, yields a return power that is ≈300,000 times smaller for a 3-mm radar (used in this study) than for a 10-cm radar (Equation A4 in Knight and Miller 1998). Thus CBL angel echoes observed with a millimeter-wave radar are almost exclusively caused by insects (Campistron 1975).

Our observations in the central Great Plains confirm that a rapidly moving, sensitive millimeter-wave radar can "see," not only radar fine-lines associated with convergence zones, but also numerous rather well-defined echo plumes remote from large-scale atmospheric convergence zones such as fronts. Shown in Fig. 2a is a sample transect of radar reflectivity across a section of CBL. The black belt is the radar blind zone; the aircraft can be seen descending to near ground level. The WCR antennas profile the atmosphere below and above the aircraft as it flies through the middle of the blind zone. Several echo plumes can be seen.

The radar reflectivity η (m^{-1}, generally shown in dBη units, 10logη) is defined as:

$$\eta = \sum n(\sigma)\sigma \qquad [1]$$

Here, σ is the scattering cross-section (echoing area; m^2) of the targets, $n(\sigma)$ is the density or concentration (m^{-3}) of targets with a given cross-section σ, and the summation is over all scatterers in a unit of volume of air observed by the radar. That volume is a function of the radar pulse width, which determines the along-beam resolution, and the radar beam width, which determines the diameter of the radar signal cone. That diameter increases linearly with range. For the WCR, the beam width angle is 0.7°, and the along-beam resolution is either 15 or 30 m. Thus, for the radar ranges used here, the unit of volume of air is 30 by 30 by 30 m or smaller.

The relationship between the scattering cross-section and the physical cross-sectional area of the insects depends strongly on size of the insects relative to the radar wavelength λ, which is 3 mm for the WCR. An experimental relationship between scattering cross section and insect mass has been shown in Riley (1985; their Fig. 4) and Russell and Wilson (1997; their Fig. 4). This relationship is compared with the theoretical scattering efficiency of spherical water droplets. The scattering efficiency is the ratio of the scattering cross-section σ to the physical cross-section. The relationship shows that at X-band (3 cm), the scattering ef-

ficiency increases with about the fourth power of size for insects lighter than ≈100 mg (≈10 mm in diameter). In other words, microinsects scatter similarly to water droplets in the Rayleigh regimen. Thus, in the Rayleigh regimen, σ is proportional to the sixth power of diameter D (D^6) (i.e., D^4 times insect surface area). Macroinsects are in the Mie regimen at X-band: their scattering efficiency changes little with size. Thus X-band radars are far more sensitive to macroinsects than to microinsects. Hardy (1968) calculates that, if insects were 2.5 mm in diameter (water sphere equivalent), an abundance of 1 insect/300 m^3 would be required in insect plumes to explain the observed reflectivity at X-band. For a 3-mm radar, the insect size that marks the boundary between Rayleigh and Mie is 10 times smaller, ≈1 mm (0.1–1.0 mg in weight). Most microinsects (including most aphids) exceed that size; thus, most microinsects scatter significantly, at the Mie threshold, and only the smallest insects scatter much less in the Rayleigh regimen. Thus, if the combined cross-sectional area of all microinsects in the CBL exceeds that of macroinsects, the CBL echoes seen in Fig. 2a are largely caused by microinsects.

Assuming, for instance, that the plumes are populated by aphids with a body mass of 10 mg, the 95-GHz (3 mm) scattering cross-section is 10^{-6} (Russell and Wilson 1997) to 10^{-7} m^2 (Riley 1985). A radar reflectivity of −85 dBη in the background corresponds to an aphid concentration of one aphid per 30–300 m^3, whereas a reflectivity of −65 dBη, as found in some plumes, would give a concentration of one aphid per 0.3–3 m^3, i.e., 100 times larger. This roughly agrees with several observations reported in Vaughn (1985). Schaefer (1976) and Rainey (1976) described typical densities of insects with an X-band scattering cross-section of 10^{-7} to 10^{-4} m^2 in Africa. They report ≈1 insect/1,000 m^3 in the background and 10–100 insects/1,000 m^3 in radar fine-lines in Africa. Wilson et al. (1994) and Russell and Wilson (1997) found that radar fine-lines have a reflectivity of 10–30 dBη above the background for precipitation radars. This corresponds to insect concentrations in the fine-line that are one to three orders of magnitude larger than in the background, assuming identical size distributions (Riley 1999). The CBL reflectivity variations at S-band may be caused by differences in size distributions (a few large insects, ≈30 mm in diameter, may dominate the signal). A W-band radar is less sensitive to insect size variations because most insects have the roughly same scattering efficiency. Thus, observed reflectivity variations in the CBL must be caused by differences in insect concentrations.

In short, insect concentrations may be as high as 1 insect/m^3 in the plumes seen in Fig. 2a and 1 insect/100–1,000 m^3 in the background. This is consistent with the observation that most WCR sample volumes, which are 100–1,000 m^3 in size at a range of 200–600 m, contain a measurable echo even between plumes. An analysis of data for 29 May in western Oklahoma shows that ≥80% of the full CBL profile is detected in about one-half of the profiles.

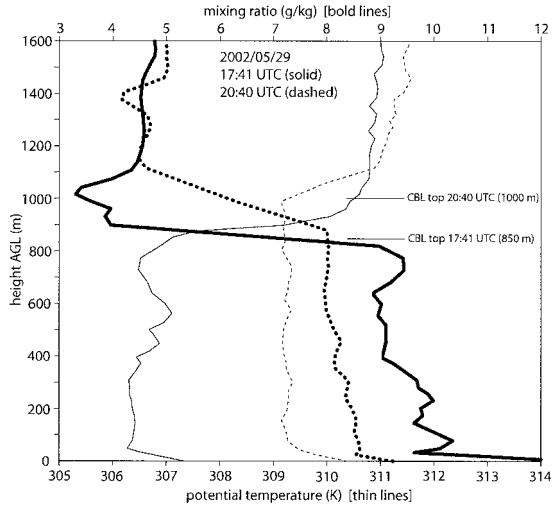

Fig. 3. Profiles of potential temperature (thin lines) and water vapor mixing ratio (bold lines) as measured by radiosondes released ≈3 h apart on the western track. The CBL top corresponds with the base of the large gradients. The lowest air temperature, just below the CBL top, is 17.8°C (18.4°C) in the 17:41 UTC (20:40 UTC) sounding. The profile of wind speed and direction at 17:41 UTC is shown on the right, using a meteorological convention: a full barb is 5 m/s. The local solar noon is at 18:40 UTC.

Depth of the CBL as Defined by Insect Plumes. Above the CBL, the microinsect concentration decreases rapidly. In fact, the insect density can be used to infer the depth z_i over which thermals occur (Fig. 2a). We define z_{i_WCR} as the level where the mean reflectivity and signal-to-noise ratio both decrease rapidly. To ascertain that the z_{i_WCR} corresponds to the top of the CBL, we compared it to the thermodynamically defined CBL depth (z_{i_TH}). The latter is the base of a layer in which potential temperature (θ) rapidly increases, and water vapor mixing ratio (q) decreases. The variables θ and q are conserved in the absence of heat or moisture sources, so they tend to be fairly uniformly distributed by the turbulence in the CBL, but they can change during the daytime, mainly on account of surface heat and water vapor fluxes, at least on quiescent days such as those examined here. Thus in a well-mixed CBL, θ is constant with height, which implies that the air temperature decreases at 10°C/km. The profiles of θ and q, measured by a radiosonde released at 1741 universal time coordinate (UTC; ≈1 h before local solar noon) along the flight track on 29 May 2002 (Fig. 3), show a well-mixed CBL and a well-defined CBL top near 850 m. Another sonde released 3 h later indicates that the CBL has warmed and deepened by some 150 m. The potential temperature jump at the CBL, which is a measure of how well the CBL is capped, is only ≈2 K at 2040 universal time coordinate (UTC), but no thunderstorms developed that afternoon. The transect in Fig. 2 is ≈20 km north of the 1741 UTC sounding in Fig. 3 and nearly 20 min earlier. Precise time-space matching is important in some cases, such as on 29 May. A

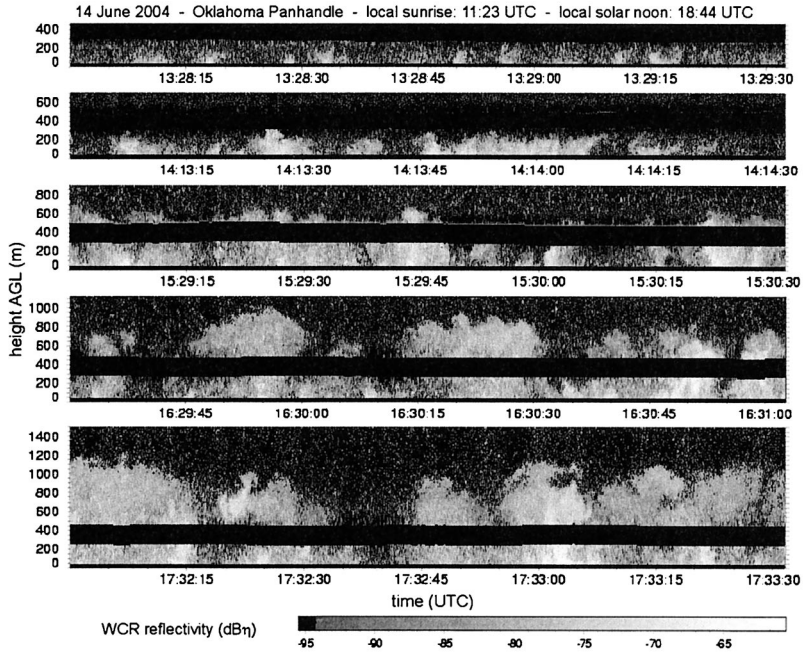

Fig. 4. WCR reflectivity transects depicting the development of the CBL on a calm, sunny morning in the central Great Plains on 14 June 2002. All cross-sections have a 1:1 aspect ratio.

comparison between Figs. 2a and 3 suggests that z_{i_WCR} is a few hundred meters higher than z_{i_TH}. A reflectivity transect further south, over the radiosonde site, at 1740–1744 UTC, does show a z_{i_WCR} in good agreement with z_{i_TH}, between 800 and 900 m AGL. The reason for the slope in CBL depth, from south to north along the western track on 29 May 2002, is believed to be a soil moisture gradient (LeMone 2003). Up to 80 mm of rain fell in the southern portion of the western track during the 24 h ending at 12 UTC on 28 May, resulting in saturated soils and a CBL depth less than that further north.

A more rigorous comparison was conducted for this and three other cases, using transects, as shown in Fig. 2a, and thermodynamic profiles obtained from nearby radiosondes or from aircraft sondes, flown regularly from the surface to some 500 m above the CBL. The average depth z_{i_WCR} for these four cases is 1,220 m, and the average difference ($z_{i\_WCR} - z_{i\_TH}$) is +90 m, ranging from −30 to +220 m. This uncertainty is consistent with the variability in CBL depth, ranging from overshooting thermals to depressions in which dry, warm air from aloft may be entrained into the CBL. It is possible that microinsects sometimes penetrate and remain in the stable layer that caps the CBL, so that a thin band of enhanced reflectivity is found in that layer.

In short, the insect-based CBL determination corresponds well with the true, thermodynamic CBL depth. This implies that the WCR scatterers are clearly trapped in the CBL and thus are weakly flying.

Insect Plume Characteristics. The insect plumes are often remarkably well defined. Most plumes cover the entire depth of the CBL. Some emerge from near the ground, are well-defined, but have not reached the CBL top. Data from three flight missions, flown along a 50-km long racetrack from sunrise to noon, indicate that the plumes grow as the CBL deepens, as first documented by Konrad (1970). Sample transects from one of these is shown in Fig. 4. Late-afternoon flights on all tracks show that the CBL remains marked by insect plumes until ≈ 4 h after local solar noon. After that time, plumes weaken and the echo strength fades, in concordance with the observed weakening of the vertical velocity and buoyancy signature of thermals. This means that insect plumes persist for ≈8 h, at least in late spring in the central Great Plains. Of course individual insects may not stay aloft for nearly that long. It is more likely that the CBL is populated by successive streams of insects. The diurnal cycle of microinsects in the CBL seems to be consistent with that in the surface layer, the lowest 10 m of the atmosphere, where tower measurements are possible. The microinsect frequency is bimodal in the surface layer, with peaks shortly after dawn and in the late afternoon (Johnson 1969, Isard and Irwin 1993). The minimum in between is caused by a net movement of microinsects into the deeper CBL.

Plumes have a height that roughly corresponds to their width. This 1:1 width-height ratio is roughly maintained during the development of the CBL (Fig. 4). However, plumes are irregularly shaped and spaced. To characterize plumes somewhat quantitatively, we defined them as regions of radar reflectivity at least 1 dB above the background and at least 200 m wide. The definition of a plume clearly must involve

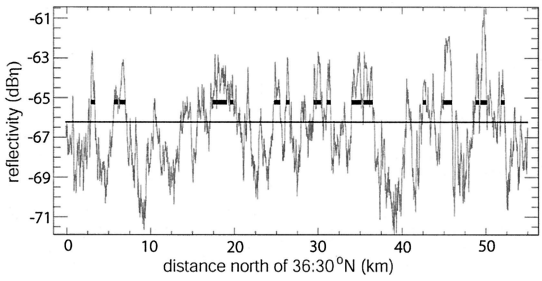

Fig. 5. Sample trace of radar reflectivity along a flight leg near 500 m AGL between 1809 and 1821 UTC on 29 May 2002. The reflectivity η shown here is the average value over a depth of 120 m above and 120 m below the radar blind zone. The horizontal line is the average for this entire trace. The short bold lines at 1 dB above this average indicate the insect plumes. These are defined as regions with a reflectivity of at least the average plus 1 dB over a distance of at least 200 m. All reflectivity averaging occurs in η units, not dBη units. Some plume statistics for this flight leg are listed in Table 1.

a width criterion, because individual radar profiles are only a few meters wide at close range to the aircraft and because numerical simulations (e.g., Mason 1989) and laboratory experiments have shown that CBL thermals have a width comparable to their depth. Looking at cross-sections such as in Fig. 2a, we can identify plumes, because the eye tends to filter out the fine-scale variability to focus on larger plumes. Therefore, we low-pass filtered the reflectivity, such that only wavelengths >200 m are retained. That minimum width was imposed to make the vertical dimension of plumes average comparable with the horizontal one.

An example of a trace of reflectivity is shown in Fig. 5. Here, the reflectivity is averaged for eight gates (120 m) above and eight gates below the aircraft. The centering of these data at the aircraft flight level allows comparison with aircraft-based measurements. Thus defined, ≈15–26% of the CBL is considered plume, and the remainder of the CBL is background (Table 1). These plumes have an average reflectivity of 4.3 dB above that of the background. That implies that plumes have nearly three times as many insects as the background, assuming that the insect size distribution is the same inside and outside of plumes.

Plumes, marked by horizontal bars in Fig. 5, can be seen to be irregularly sized and spaced. Plumes are 600 m wide on average (Table 1), but the SD is large (336 m for all flight legs). Their width tends to increase a little as the day progresses past local solar noon, and late-afternoon plumes are less well-defined, i.e., their reflectivity excess above the background is smaller. The spacing between plumes averages between 2.4 and 3.0 km, but that too is quite variable, as seen in Fig. 5.

Ignoring for a moment the existence of insect plumes, we examined the average vertical profile of radar reflectivity. Figure 6a shows that, on average, reflectivity decreases with height in the CBL at a rate of ≈10 dBη/km. This suggests that more insects are found at low levels and/or that on average the low-level insects have a larger scattering cross-section. Airborne trapping studies (Johnson 1957, Glick 1960, Isard et al. 1990) confirm that the average insect density decreases with height in the CBL and that the density variation with height can be described empirically by an inverse power law. This implies that the logarithm of the insect density decays linearly with height, and thus, reflectivity (in dBη units; see Fig. 2a) should also linearly decay. This vertical profile seems to be confirmed by the probability density function in Fig. 6a. Clearly, the average vertical variation of insect concentrations ignores the remarkable horizontal variation (e.g., Figs. 2 and 4), which is more pertinent to this study.

Insect Plumes and Updrafts. We examined whether insect plumes generally correspond with updrafts. The vertical air currents are measured by means of a gust probe on a boom that sticks out from the nose of the aircraft (see *Vertical Air Velocities*). The reflectivity

Table 1. Plume statistics for 10 flight legs on 29 May 2002 along the western track

Flight leg times (UTC)[a]		z_{i_WCR}[b] (m)	Fight level[c]/ z_{i_WCR}	N. of plumes	Plume width		Mean plume spacing (m)	Fraction of CBL plume[d] (%)	Vertical velocity excess[e] (m/s)	Reflectivity excess[f] (dB)
Start	End				Mean (m)	SD (m)				
1655	1708	907	0.70 (H)	20	459	180	2,501	15	0.67	3.4
1711	1723	996	0.34 (M)	18	437	252	2,586	15	0.72	3.5
1725	1739	972	0.18 (L)	19	653	482	3,027	18	0.19	3.6
1755	1807	1,106	0.81 (H)	26	729	327	2,160	24	0.36	4.4
1809	1821	1,093	0.39 (M)	19	574	281	2,507	22	0.76	3.6
1823	1837	1,167	0.13 (L)	27	568	256	2,605	22	0.14	3.7
1840	1851	1,109	0.80 (H)	19	691	383	2,458	25	0.52	5.1
1853	1907	1,023	0.41 (M)	25	546	437	2,771	26	0.97	4.9
1909	1921	1,054	0.10 (L)	24	548	257	2,422	23	0.24	4.8
1924	1937	1,005	0.86 (H)	19	773	502	2,948	24	0.53	5.5

[a] The flight legs are identified by their start and end times; the local solar noon is at 1840 UTC.
[b] z_{i_WCR} is the CBL depth as determined by radar reflectivity.
[c] This is the average flight level, as a fraction of the CBL depth. Each flight leg was relatively level. H, high-level; M, mid-level; L, low-level.
[d] This is the fraction of the radar profiles considered to be in-plume on the flight leg.
[e] This is the gust-probe measured vertical air motion excess in the plumes over that in the background between plumes.
[f] This is the radar reflectivity excess in the plumes over that in the background between plumes.

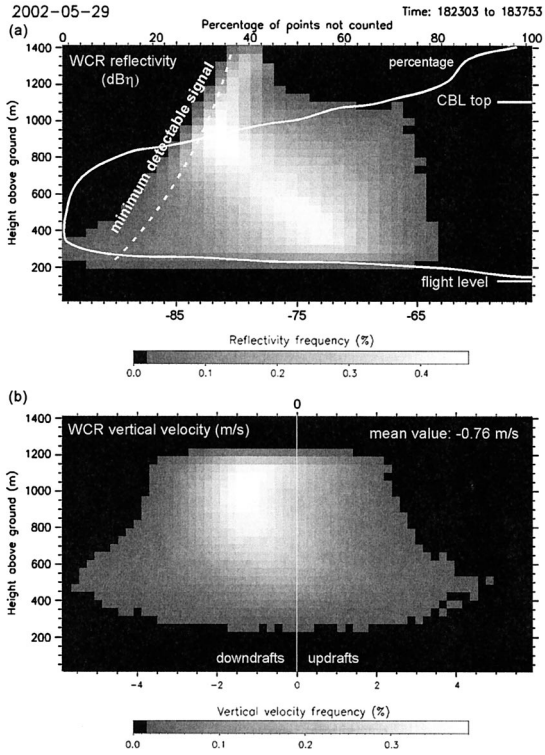

Fig. 6. Probability density function (or 2D histogram) of (a) reflectivity and (b) WCR velocity for a sample flight leg (the 1823–1838 UTC leg on 29 May 2002). The frequency is normalized, i.e., the sum of the occurrences at all heights and for all values equals 100%. The flight level is 65 m AGL on average; therefore, only radar data above the aircraft are included. Also shown in a, as a dashed white line, is the minimum detectable radar signal, which is range dependent. The white line in a shows the percentage of the CBL not sampled. This percentage approaches 100% near the CBL top, because the return signal is too weak there, and at low levels, because of the blind zone around the aircraft.

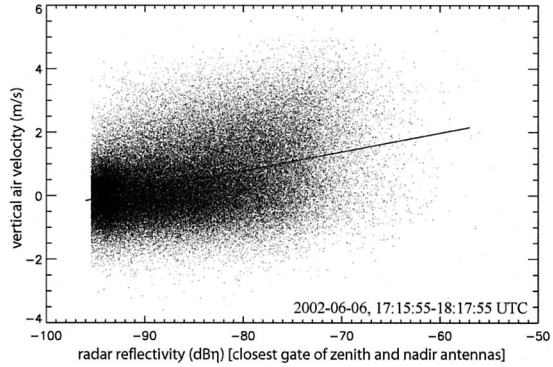

Fig. 7. A scatter plot of vertical air motion, as measured by the gust probe aboard the aircraft, versus radar reflectivity, for 62 min of flight data on 6 June 2002. Given a sampling rate of 30 Hz (3 m along the flight track), about 10^5 observations are shown. The reflectivity estimate comes from just above and below the aircraft, so geometrically, the average is centered at flight level.

shown in the scatter plot of Fig. 7 is the average of the values in the first radar gates above and below the aircraft, 225 m apart. Clearly, a lot of scatter exists in the relationship between vertical air motion and reflectivity, in part because of the spatial separation between velocity and reflectivity measurements and the intense turbulence in the CBL. Instead of the gust probe vertical velocity, the Doppler velocity could be used at the same gates as the reflectivity data, but that velocity may be biased by insect motion. The positive correlation evident in Fig. 7 indicates that plumes of higher reflectivity tend to correspond with updrafts.

To reduce the scatter, we binned the radar reflectivity by 1-dB intervals and computed the average vertical air velocity for each reflectivity bin. This average vertical air velocity increased with increasing reflectivity on three different flights (Fig. 8), except perhaps for the highest reflectivity values. The total number of samples on each of the three flights summarized in Fig. 8 can be computed as the number of minutes times 1,800, i.e., the number of samples per minute. The number of samples per reflectivity bin decreases with reflectivity, so the relationship shown in Fig. 8 becomes less certain for high values of reflectivity, especially above −72 dBη. Also, some high nadir-beam reflectivity values may be contaminated by objects sticking out above the ground (trees, antennas, etc.) where the flight level is ≈150 m above ground level. Data from lower flight levels (Table 1) are all excluded because the first gate in the nadir antenna is strongly contaminated by the earth surface.

The average vertical air motion on each of the three flights shown in Fig. 8 is <0.1 m/s. This may not seem to be the case from Fig. 8, but it should be remembered that the largest number of samples occurs at the lowest reflectivities, where downdrafts prevail. Table 1 compares the vertical air motions within these plumes to that of the background for one of the three flights shown in Fig. 8. Insect plumes tend to correspond with updrafts in all flight legs, and vertical air currents in plumes exceeded that of the background by an average of 0.51 m/s. Buoyant thermals tend to accelerate upward, so it is not surprising that the vertical velocity excess in plumes is rather small at low levels (Table 1). For the seven mid- and upper-CBL flight legs in Table 1, the average vertical velocity excess in plumes is 0.65 m/s.

Vertical Motion of Microinsects in the CBL

The airborne radar configuration used in this study enables us to remove the vertical air motion from the radar-derived vertical motion to obtain the insect motion relative to the air. The vertical air motion, denoted as w_a, is measured by the gust probe on the aircraft. We denote the WCR nearest-gate zenith and nadir beam velocity as w_{r_up} and w_{r_down}, respectively, and their average as w_r. The WCR data obviously are displaced from the aircraft, but w_r is centered within 20 m of the flight level. The 225-m blind zone (Figs. 2 and 4) may be argued to be rather deep for such linear

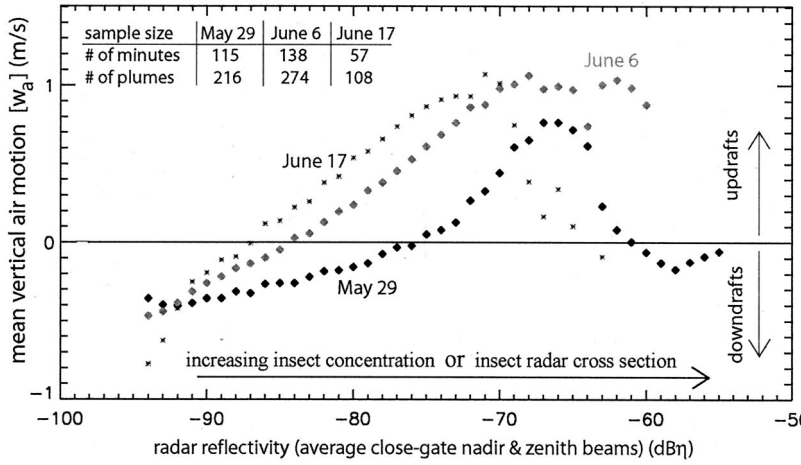

Fig. 8. Mean vertical air motion for each reflectivity bin on three different flights. Also listed are sample size statistics and overall mean vertical air motion.

interpolation, but plume-scale vertical velocity cores can be seen to be rather continuous across this zone (Figs. 2 and 6).

How Accurate are Vertical Velocities from Radar? The vertical velocity shown in Fig. 2b is derived from the WCR Doppler velocities, after removal of the Doppler velocity components caused by aircraft vertical motion and by departures from the exact nadir and zenith orientations caused by aircraft roll and pitch (Leon and Vali 1998). It is easy to conceive that a small radar beam pointing angle error, say forward from nadir, will cause a false Doppler movement of the insects toward the aircraft, on account of the aircraft forward speed. Moreover, the aircraft flies in a turbulent environment, so its attitude changes rapidly. Therefore, much effort went into the correction of the radar Doppler velocities for aircraft motion changes and into the validation of these corrections.

One question is in regard to the exact pointing angle of the nadir and zenith antennas. This question can be assessed by means of the average WCR velocity at the range corresponding with the earth's surface. If the nadir antenna points slightly forward, the earth's surface will be moving toward the radar at a fraction of the aircraft speed. That fraction is geometrically related to the offset from vertical, and such assessment resulted in a correction of the antenna position early on during the field campaign. The average vertical velocity of the earth's surface (w_{wcr_g}) for the three flights analyzed here is <0.1 m/s (Table 2). The average is computed for all straight and level CBL flight legs during which nadir WCR data were collected on any flight. The flight legs are flown in opposite direction, so the impact of the mean along-track wind on radial velocities would be cancelled. Slight net off-vertical orientations of the nadir beam do occur during flight, depending mainly on aircraft fuel weight, but the net nadir beam vertical velocity at the earth's surface (w_{wcr_g}) for any single flight leg (of all legs included in Table 2) is <0.50 m/s. For the zenith

Table 2. Summary of the comparison between radar and aircraft vertical motions

	29 May Western	6 June Central	17 June Eastern
No. of minutes	115	138	57
No. of flight legs	10	9	7
Mean w_{wcr_g} (m/s)[a]	0.04	0.04	0.03
Fraction of time with w_r data[b]	68%	89%	75%
Mean w_a where w_r exists (m/s)	−0.03	+0.02	+0.08
Mean w_{r_up} (m/s)[c]	−0.72	−0.36	−0.39
Mean w_{r_down} (m/s)[d]	−0.59	−0.35	−0.09
Mean insect response ($w_a - w_r$; m/s)	0.61	0.40	0.30
Linear regression (based on binned w_a) w_i =	$0.54 + 0.45w_a$	$0.36 + 0.50w_a$	$0.17 + 0.53w_a$
Correlation coefficient (bin-mean values)	0.97	0.99	0.96

[a] The term w_{wcr_g} is the WCR velocity, corrected for aircraft motion, at the reflectivity max corresponding to the ground; this and other averages listed in this table are calculated over the straight and level flight sections where combined up/down antenna and aircraft data are available; the total time, and the no. of flight legs, over which these combined data are collected, are listed in the third and fourth row.

[b] The term w_r refers to the average of w_{r_down} and w_{r_up}, and w_r data are available only where the WCR operated in profiling mode and only at those flight levels that were ≥200 m below the CBL top and ≥200 m above the ground.

[c] The term w_{r_up} is the WCR velocity at the first gate (105 m) above the aircraft.

[d] The term w_{r_down} is the WCR velocity at the first gate (120 m) below the aircraft.

beam, such validation is not possible, but the average nadir and zenith vertical velocities are within 0.30 m/s of each other (Table 2). The average zenith beam vertical velocities are slightly more negative for all three flights. However, the average difference between zenith and nadir antennas, 0.01–0.30 m/s, is within the variability of the true vertical air motion over a depth of 225 m (the spacing between the up and down antenna first gates) and can also be related to height-dependent flight behavior of insects within the CBL.

Because of the proximity of antenna pointing angles to the vertical, the relatively weak CBL winds, and the fact that the tracks were flown repeatedly in both directions, any systematic contamination of the horizontal air or insect motion into the vertical is negligible. In short, the uncertainty of w_r is $\approx$0.2 m/s.

How Accurate Are the Vertical Air Velocities?. The vertical air motion is estimated at flight level from the aircraft gust probe. The procedure is rather standard (e.g., Miller and Friesen 1985). The temporal resolution of 25 Hz, or $\approx$4 m in the along-track direction, is roughly the same as that of the WCR profiles. The gust probe vertical velocity is believed to be accurate to at least 0.50 m/s for instantaneous measurements (A. Rodi, personal communication). For long flight legs (50 km), slight errors in the vertical accelerations measured by the inertial navigation system may lead to a error in mean vertical air velocity of up to 0.5 m/s. Over the long flight legs used here (45–60 km), the mean vertical motion should be close to zero (at least $<$0.10 m/s), because fair-weather conditions prevailed. Thus, the average gust probe vertical velocity over the length of the straight flight tracks used here is set to zero. This velocity will be referred to as "vertical air motion" (w_a), and the term "updraft" ("downdraft") refers to the condition $w_a > 0$ ($w_a < 0$). w_a has an uncertainty of $\approx$0.1 m/s.

Microinsect Vertical Motion in Down- and Updrafts. The CBL plumes generally contain updraft cores, yet the WCR data, from both the up and down antennas, indicate that subsidence prevails. This is evident in Fig. 2b as a dominance of dark shades over light ones. Along one flight leg on 29 May, subsidence clearly prevails at all levels (Fig. 6b), which immediately invokes the question of how microinsect concentrations in the CBL can be sustained. This is the key question of this study, as mentioned before.

The mean rate of subsidence in the case shown in Fig. 6b (0.76 m/s) is almost as large as the SD of the velocity distribution. This subsidence appears at all levels: there is no clear dependence on height within the CBL (Fig. 6b). When only the stronger echoes ($>$ -75 dBη) are sampled, the bulk of the radar scatterers still sink, but the average rate is slightly less (0.60 m/s). Such vertical motions are not found in the gust probe data (Table 2), suggesting that the scatterers (i.e., the insects) tend to move down against the current.

The difference between aircraft and radar vertical velocities, $w_a - w_r$, is referred to as the insect response (w_i), because it can only be attributed to insect vertical motion relative to the air. Such response can be realized in many ways: insects can actively fly down, they can passively fall down with their wings folded, or they can fall with their wings unfolded. The latter is the slowest; which of the former two methods is the fastest depends on the Reynolds number, which depends on the size of the insect, which is probably limited to 1–2 m/s, depending on microinsect species (Pedgley et al. 1982). We will assume that the insect response (upward or downward) does not exceed 1.5 m/s.

The measurement uncertainty of the mean insect response is determined by that of the w_r and w_a averages, which have been discussed above. The root mean square of both uncertainties is $\approx$0.2 m/s for long-track averages. Part of the CBL is not sampled (Fig. 6a), but we calculated the insect response based only on profiles where both w_{r_up} and w_{r_down} were available. About 89% of the 29 May profiles in the 115 min with both up and down antennas in operation have w_r values.

To be significant, a large number of flight legs need to be compared, and the resulting scatterplot of w_a versus w_r values, sampled at high frequency (every 0.04 s), looks like a dark cloud that reveals little correlation (Fig. 7). Therefore, we binned the w_a values in 0.2-m/s increments. We built each bin with w_r values during a period of 1 min (i.e., a flight track of 5 km), during which $\approx$1,800 profiles were collected. We next calculated the mean w_r value in each w_a bin. Note that vertical velocities are not averaged over 1 min. It is obvious from Figs. 2 and 4 that several cells are traversed in 1 min; therefore, that average would be small. Rather, instantaneous w_r values were placed in bins, depending on the corresponding value of w_a, and after 1 min, all w_r values in a given bin were averaged. Mean w_r values are shown in Fig. 9 for 115 such time segments collected on the 29 May flight. Clearly, not all w_a bins will be equally populated. The scatter of mean w_r values broadens toward extreme values of w_a because the average w_r is based on just a few measurements out of the total of 1,800, sometimes just 1. The w_a distribution appears close to normal, with a mean value of -0.03 m/s (Table 2) and a slight positive skewness.

The mean w_r value corresponds reasonably with the w_a bin value in downdrafts, where insects tend to subside with the air current (Fig. 9): in the downdraft region alone ($w_a < 0$), the regression slope is close to unity (0.81). However, in updrafts ($w_a > 0$), w_r lags behind significantly (Fig. 9), suggesting that insects respond to being lifted. For instance, in a 1.0-m/s updraft, insects head down at 1.0 m/s on average, according to the regression line shown in Fig. 9. Clearly, insects tend to descend, and the stronger the updraft, the more they oppose it. In downdrafts, this opposition fades.

Average Vertical Flight Behavior of Microinsects. All w_r values for each w_a bin shown in Fig. 9 can be averaged. These average w_r values, or the corresponding insect response ($w_a - w_r$), are strongly related to w_a itself (Fig. 10). The relationship between the average insect response and w_a is surprisingly linear, and

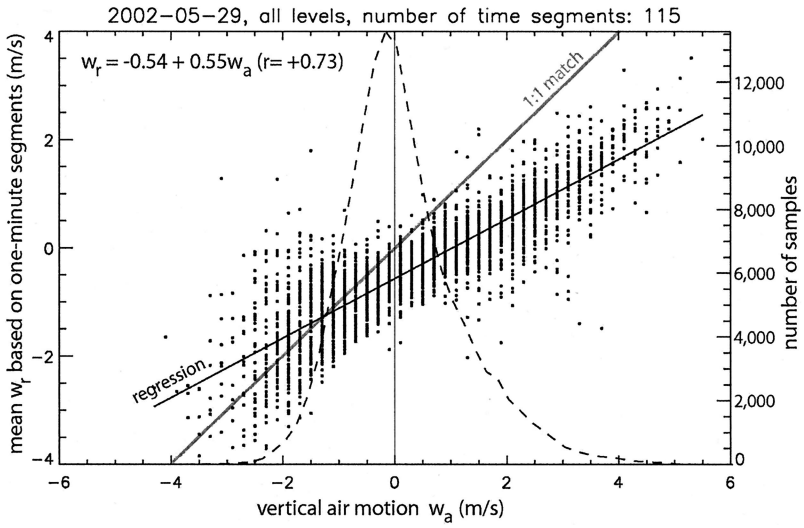

Fig. 9. The dots represent the radar (i.e., *insect*) vertical velocities (w_r) for a range of values of aircraft gust probe (i.e., *air*) vertical motions (w_a), binned in 0.2-m/s increments, for 115 1-min time segments on 29 May. Each dot represents the average of all w_r values encountered in a given w_a bin over the course of one time segment (≈1,800 samples). The dashed line is the distribution of w_a values coincident with radar measurements.

the linear correlation coefficient is remarkably high (0.97 for the 29 May data; Table 2). On 2 other d, 6 June and 17 June, at different tracks (the central and eastern track, respectively; Fig. 1), a very similar strong linear relationship emerged between the average insect response and w_a (Fig. 10). The linear dependence of the insect response w_i on w_a, averaged over three flights (each weighted by the number of 1-min samples listed in Table 2), is as follows:

$$w_i \equiv w_a - w_r = 0.42 + 0.49w_a \quad [2]$$

On average, for all data on three flights, insects move down relative to the ambient air at a speed of 0.45 m/s. The regression equations and mean values for the three flights are listed separately in Table 2.

The linearity of the response, and its reproducibility, suggests the possibility that this is some artifact of the measuring systems or the method of correcting for

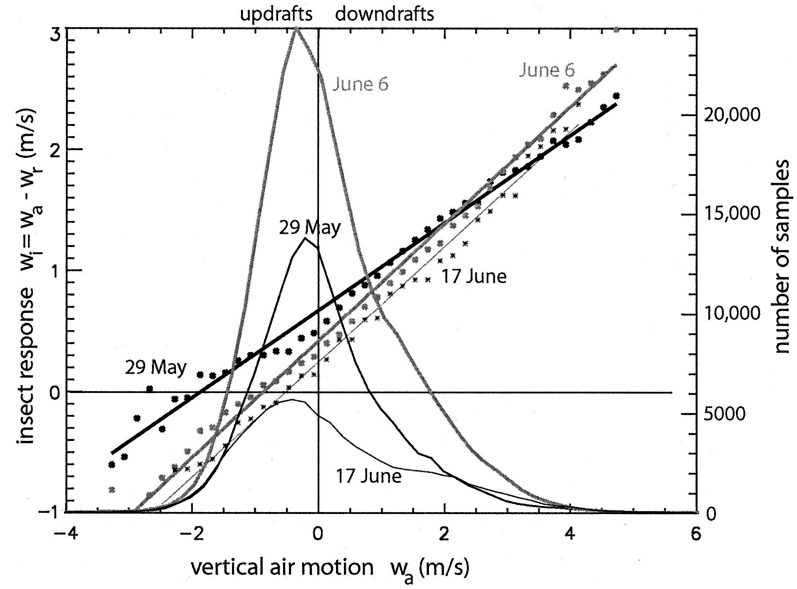

Fig. 10. Regression curves (straight lines) and observed mean insect response ($w_a - w_r$) values (stars and dots) as a function of vertical air motion w_a (binned in 0.2-m/s increments) for three flights, and their respective distributions of w_a measurements (curved lines). The regression equations and correlation coefficients for these three flights are listed in Table 2.

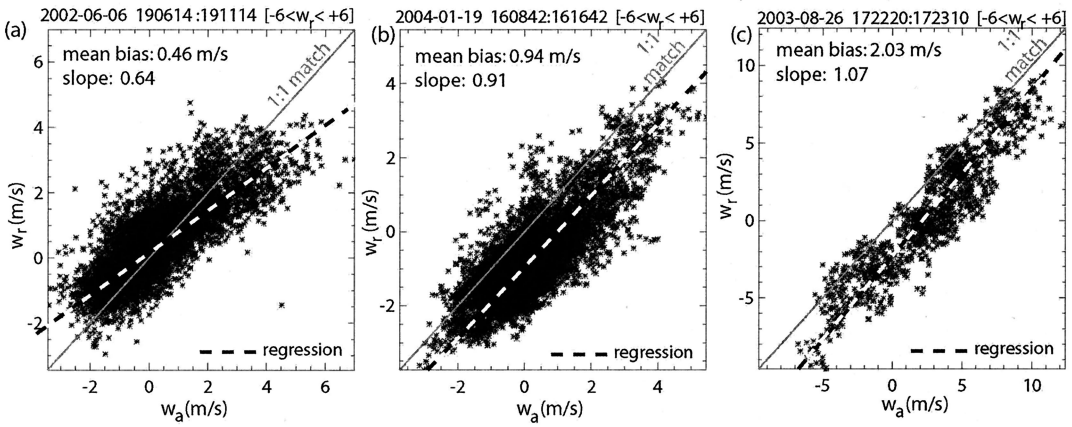

Fig. 11. Linear regressions of w_r versus w_a for sample flight legs (each 20–50 km long) in three very different situations. The scatterplot values are neither averaged nor binned. (a) The scatterers are insects in a cloud-free CBL. The flight leg occurred on 6 June 2002 on the "central track" in Kansas at 0.6 km AGL. (b) The scatterers are small snowflakes in a cloudy CBL over a Lake Michigan. The flight was conducted during a cold-air outbreak on 19 January 2004 at 0.5 km AGL, with air temperatures around −15°C. (c) The scatterers are rimed ice particles in a cumulus congestus cloud at 5.5 km MSL, well above the CBL. The flight took place on 26 August 2003 in Wyoming.

aircraft motion. Independent checks have confirmed the accuracy of radar-derived velocities. More convincing perhaps is the observation that the regression slope between w_r and w_a in the optically clear CBL is between 0.47 and 0.55 in Fig. 9 and on other days (Table 2; note that if $w_a - w_r = a + bw_a$, where a and b are constants, as in Table 2, then $w_r = -a + [1 - b]w_a$). The highest regression slope on any individual flight leg is 0.64 (Fig. 11a). This stands in contrast with observations in cloud (Fig. 11b and c). The clouds on which Fig. 11b and c are based were sampled as part of two separate research efforts, but using the same aircraft, the same radar configuration, and the same processing methods. In the case of Fig. 11b and c, the difference $(w_a - w_r)$ is 0.9 and 2.0 m/s, respectively. This difference corresponds well with the fallspeed (terminal velocity) of the hydrometeors, which were sampled by particle probes aboard the aircraft. Unrimed snowflakes (Fig. 11b) fall at ≈1 m/s, whereas rimed ice crystals in cumuli congesti (Fig. 11c) fall at ≈2–3 m/s. The key is that the regression slope between w_r and w_a is close to 1.0; the fall-out is independent of updraft strength. Very similar results are found along other flight legs in Wyoming cumuli congesti and in shallow snowbands over Lake Michigan: for all legs, the regression slope between w_r and w_a falls within 20% of 1.0. None of the regression slopes in clouds are even close to those in the clear warm-season CBL, so the difference between biotic scatterers in the CBL and hydrometeors in clouds is unambiguous. Clearly, the response of the biotic scatterers cannot be reproduced in clouds using the same measuring and processing method.

One detail worthy of some attention is that, in very strong updrafts, there is no indication of a ceiling of the insect response, at least not on the 3 d sampled here (Fig. 10). A ceiling is to be expected if the scatterers are mostly weak flyers. This finding should be treated with caution, however, because the sample size is small. To sample more strong updrafts, we also evaluated the insect response for two flight legs across a mostly stationary front in the Oklahoma Panhandle in the afternoon of 3 June 2002 (data not shown). The front appeared as a fine-line on ground-based radar reflectivity maps. In this case, the mean insect response was 0.54 m/s, and the linear regression was close to the three others in Fig. 10.

Variation of Insect Response with Echo Strength and Height in the CBL. We examined the variation of the insect vertical motion with altitude within the CBL and with echo strength. Insects tended to oppose updrafts a little more vigorously at low levels than in the upper CBL on 6 June (Fig. 12). The same is true on 29 May and 17 June (data not shown), but the low-level regression line is slightly more level. Possibly, the larger reflectivity values in the lower CBL (Fig. 6a) are the result of larger insects there, which may be able to oppose updrafts more effectively. In any event, the rate of opposition displayed by insects is essentially independent of height in the CBL. This is evident also in the full-profile probability density function of WCR velocities (Fig. 6b).

The tendency of insects to descend is further examined as a function of radar echo strength (Fig. 13). Insect plumes tend to occur in updraft regions (Table 1; Figs. 7 and 8). The higher echo strength in these plumes can be caused either by a larger insect concentration or by larger insects, at least insects with a larger scattering cross section (Equation 1). Insect opposition increases slightly with echo strength on all days, except for the strongest echoes (Fig. 13). The 6 June case has more samples (Table 2), but most of the 6 June echoes are rather weak, so little can be said with regard to the stronger echoes. On 29 May, a day with stronger echoes, the relationship is similar as on

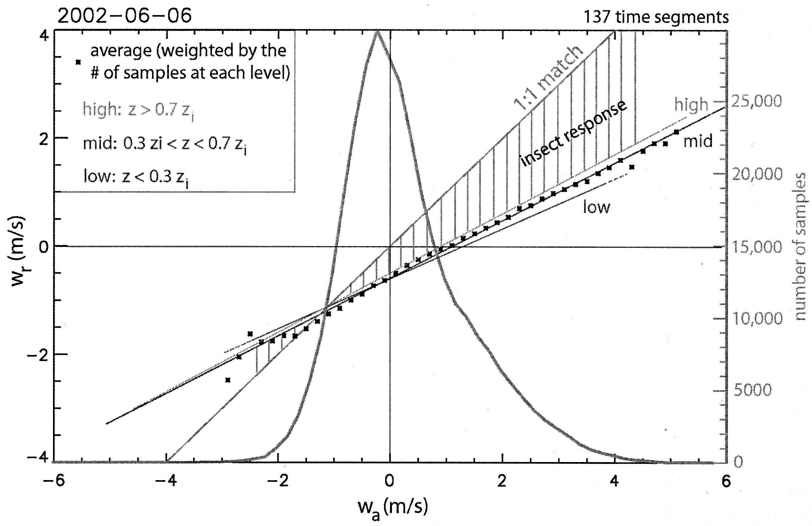

Fig. 12. Linear regressions of w_r as a function of w_a in three layers within the CBL, whose depth z_i is determined from the WCR reflectivity profile (Fig. 2). These regressions are based on 138 time segments during the 6 June flight. Also shown are the distribution of w_a measurements (solid curve) and the average w_r value at all levels within the CBL for each w_a bin (dots).

6 June (Fig. 13), but on average, the insect response is smaller (Table 2).

The slight increase of insect response with echo strength does not necessarily imply that larger insects can oppose updrafts more effectively. As discussed earlier (*Insect Plumes and Updrafts*), insects tend to be concentrated in updraft regions, and therefore the insect opposition in the plumes may be larger, simply in response to the updraft. This explanation seems more likely, given the strong correlation between insect response and updraft strength (Fig. 10), although the former explanation (that larger insects can oppose updrafts more effectively) cannot be excluded because it is impossible to separate scattering cross-section from concentration (Equation 1).

The insect response ($w_a - w_r$) remains downward (positive) for reflectivity values close to the minimum detectable signal (Fig. 13). Depending on range, much of the CBL that is undetected by the WCR (Table 2) falls in this low reflectivity region. Also noteworthy in Fig. 13 is that, at high reflectivity values (above about -72 dBη), the insect response seems to plateau and even wane. This tendency is present on all days, especially on 29 May and 3 June, when a radar fine-line

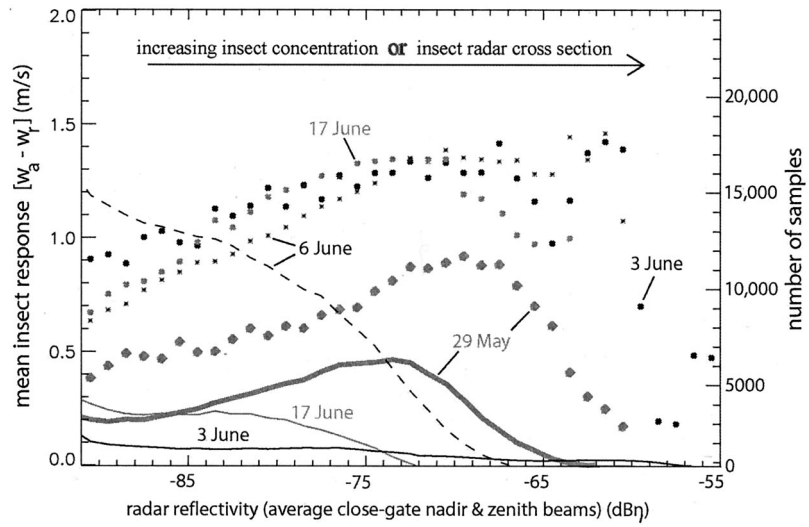

Fig. 13. Observed insect response ($w_a - w_r$; dots) as a function of coincident radar reflectivity and the distribution of reflectivity measurements (lines). The same three flight days as listed in Fig. 12 are shown, plus 3 June, a flight that focused on an insect convergence zone along a front.

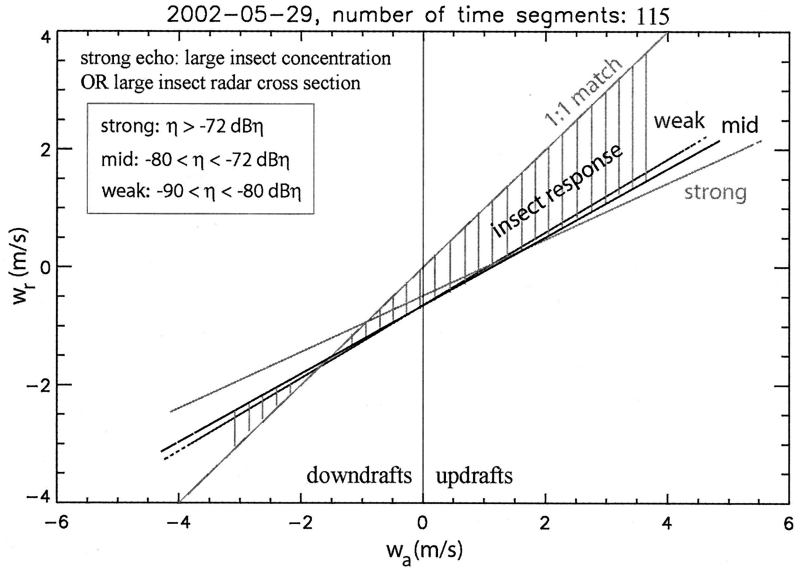

Fig. 14. The relationship between w_r and w_a stratified by echo strength for the 29 May flight.

was transected. Hypotheses can be formulated as to why the downward response would fade in the strongest echoes in the CBL, in terms of microinsect geometry or flight behavior, but we do not have evidence to support these. Certainly some of the strong echoes are not caused by insects but rather by ground clutter (see *Insect Plumes and Updrafts*). This clutter (trees, antennas, etc.) is located at random places, unrelated to thermals, so the average vertical air motion is close to zero (Fig. 8), and of course, these objects do not move, so the difference between radar and air vertical motion also approaches zero (Fig. 13).

In general, over the range where echoes are strong enough to exceed the minimum detectable signal and weak enough that they are not exceedingly rare in the CBL, the insect response is a little greater in the stronger echo regions. This is evident also from Fig. 14, where the CBL is divided into three regions according to echo strength, assuming some arbitrary reflectivity thresholds. However, again, as for the effect of height in the CBL, the dependence of insect vertical motion on echo strength is rather weak.

Extracting the Microinsect Vertical Motion from Radar Velocities. In summary, the insect response relates surprisingly strongly to air vertical motion (Table 2), irrespective of echo strength and height in the CBL. Two variables can be inferred from the WCR vertical velocity profiles in the CBL, not just at the closest radar gate but at any range from the aircraft: (1) the insect vertical motion and (2) the best-guess vertical air motion. The latter, denoted as w_{rc}, can be derived from uncorrected WCR values (w_r) at any range by means of Equation 2. That is,

$$w_{rc} = w_r + [w_a - w_r] = w_r + 0.49w_a + 0.42 = 1.96(w_r + 0.42) \quad [3]$$

because $w_a = \dfrac{w_r + 0.42}{0.51}$, according to the expression for insect response ($w_a - w_r$) in Equation 2. The best-guess vertical air motion w_{rc} (Equation 3) is used to map the insect response w_i (m/s), according to Equation 2. That is,

$$w_i = 0.49w_{rc} + 0.42 = 0.96w_r + 0.82 \quad [4]$$

The profiles of insect response and best-guess vertical air motion are shown in Fig. 15 for the same transect shown in Fig. 2. Again, these velocities have an uncertainty of ≈0.2 m/s on average. In Fig. 15b, a downward insect response ($w_i > 0$) is shown as a negative value (i.e., $-w_i$ is plotted). Also, the maximum value of w_i is set to 1.5 m/s, as discussed before (*Microinsect Vertical Motion in Down- and Updrafts*).

According to Fig. 15b, insects tend to subside in most places, but more so in updraft regions. In some places, the insects move upward; this is especially apparent in the region on the right in Fig. 15 (near 1724:30 UTC) where a downdraft seems to penetrate from aloft deep into the CBL. The downdraft regions (Fig. 15c) are still larger than the updraft regions in this and other transects we examined, and the insect response is rather neutral there (close to 0 m/s). Also, the updrafts are stronger. This is consistent with the observed skewness of the w_a distribution (Fig. 10). Most echo plumes in Fig. 15a seem to correspond with updrafts in Fig. 15c, confirming the close-gate observations discussed before (see *Insect Plumes and Updrafts*). Corrected radar (w_{rc}) and gust probe (w_a) vertical velocities concur that echo plumes tend to correspond with updrafts and that regions with peak reflectivity values near −65 dBη tend to rise at a rate of ≈1 m/s over the background of weak echoes (data not shown).

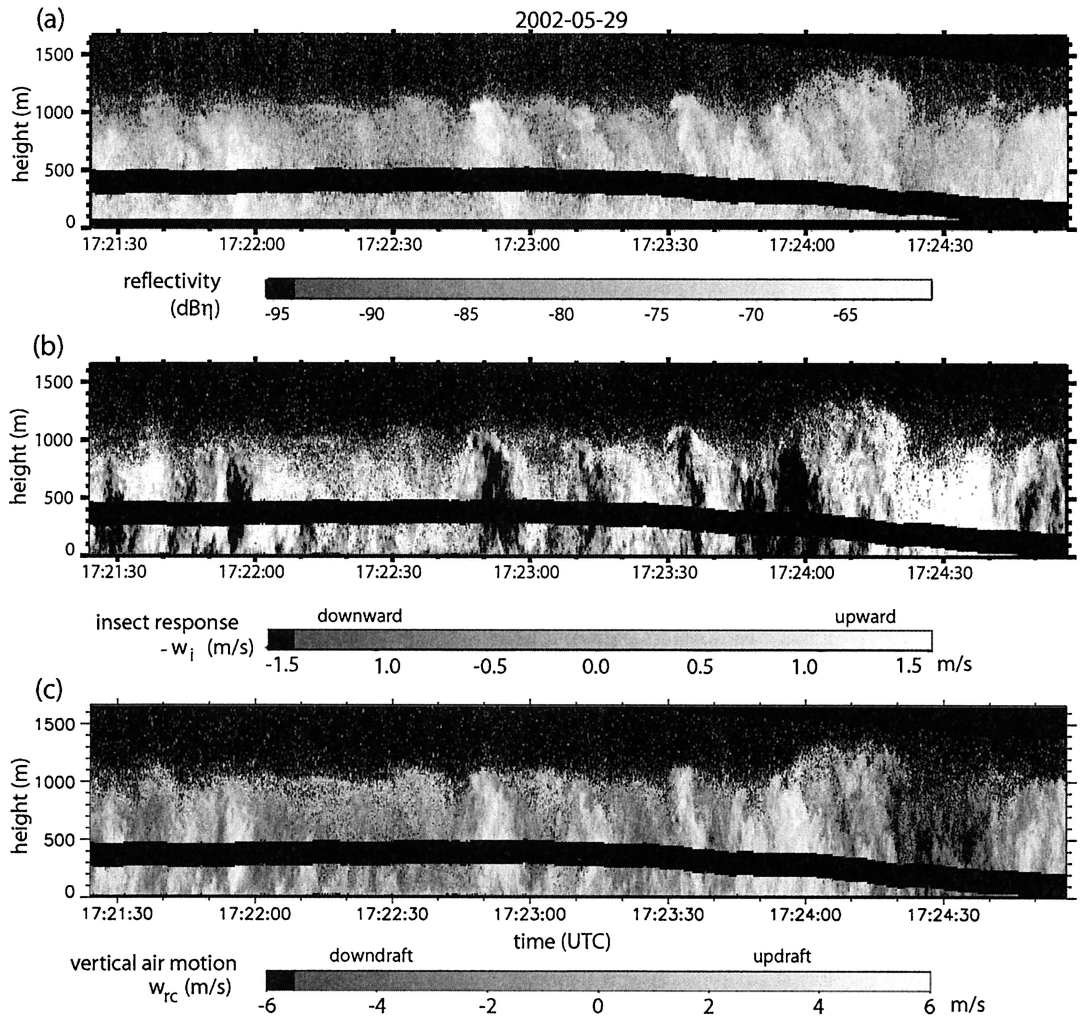

Fig. 15. (a) Radar reflectivity, as the top panel of Fig. 2. (b) Insect response w_i. (c) The best-guess vertical air motion from radar w_{rc}.

Discussion

Two key findings emerge from this study. First, microinsects tend to congregate in updrafts. Second, microinsects oppose these updrafts by active or passive downward motion. The first finding has not been directly observed before, but it has been hypothesized: higher clear-air reflectivities in radar fine-lines have been attributed to flow convergence (e.g., Drake 1982, Pedgley et al. 1982, Drake and Farrow 1989, Wilson et al. 1994, Russell and Wilson 1997), and converging currents imply rising air motion. The second finding may be surprising, as much of the aerobiological research has focused on the question of how insects, especially weak flyers, can take off and rise sufficiently to travel large horizontal distances (e.g., Isard and Gage 2001). If indeed the net motion of the microinsects is downward (we found a mean rate of subsidence of 0.45 m/s), it may be particularly puzzling how microinsects can remain aloft at all and how the CBL can be marked by insect plumes for many hours.

The second finding leads to extensive validation by means of internal consistency checks and comparison with other data sets. The possibility remains that this finding is invalid, but we cannot see how. Perhaps the insects are stunned by the passage of a noisy turbojet aircraft. Therefore they are temporarily falling down at the time that their vertical motion is measured by the radar. This, however, is unlikely because the average rate of subsidence does not decrease with increasing radar range from the aircraft. Also, there is no reason why, in this scenario, the insects would be falling faster in updrafts. In any event, we must assume that the insect flight behavior above or below the blind zone is not affected by the proximity of the aircraft.

A simple numerical simulation of insect flight behavior in a realistic flow pattern of the CBL shows that the second finding (that insects oppose updrafts) is

quite viable and that in fact it may explain the first finding (that insects congregate in updrafts). The key is that the presence of microinsects in the CBL is sustained by updrafts whose strength exceeds the rate of insect subsidence. The two findings combined then explain the existence of insect plumes and radar finelines, in which the insect concentration may be one or more orders of magnitude larger than in the background. They also explain the rapid disappearance of microinsects from the CBL in the late afternoon when the ground cools and thus buoyancy-driven updrafts disappear. The numerical modeling work and interpretation are addressed in Geerts and Miao (2005). It should be emphasized, however, that our observations apply to the ≈1-km-deep CBL only and not to the lowest 10–20 m above the canopy (the surface layer). In that layer, departing microinsects may well have to fly upward.

In conclusion, an airborne Doppler radar was used to examine the vertical flight behavior of insects in the atmospheric CBL. The CBL typically is 1 km deep and is marked by strong updrafts driven by buoyant thermals. Most scatterers are believed to be microinsects, given their concentration, their radar cross-section, and their flight behavior, although the fraction of macroinsects is unknown. The insect vertical motion is estimated by comparing the close-gate radar velocities, at ≈100 m above and below the aircraft, to the vertical air velocity, as measured by a gust probe in front of the aircraft. An error analysis suggests that the difference between these two velocity measurements is accurate to 0.2 m/s or better for long-track averages.

Our study has four basic findings. First, microinsect densities are sufficient for a high-resolution airborne 95-GHz radar to "see" most of the CBL, at least in the central Great Plains of North America in late spring. Radar observations confirm the existence of well-defined echo plumes throughout the depth of the CBL. The radar data nicely describe the growth of the CBL and associated insect plumes from the ground up during the morning hours. All this is consistent with ground-based observations reported in the literature. Second, airborne airspeed measurements, together with radar reflectivity profiles, show that insect plumes tend to be collocated with updrafts. This finding has been speculated before but never directly observed. Third, microinsects tend to subside in the CBL, at an average rate of 0.5 m/s, relative to the air. The average rate of subsidence is largely independent of echo strength or height in the CBL. Finally, the scatterers tend to oppose updrafts in which they are embedded. This opposition (measured as the difference between gust probe and radar vertical velocity) increases with updraft strength. The ability of the scatterers to respond to updraft strength is an unambiguous sign of their biotic nature.

In Geerts and Miao (2005), a simple numerical simulation of the airflow field and insect concentration in the CBL is used to confirm that the observed flight behavior (the opposition to updrafts) explains the presence of well-defined insect plumes in the otherwise well-mixed CBL and that radar echo plumes tend to be associated with updrafts. The simulation also shows that the microinsect flight behaviors cannot be controlled by air temperature alone.

Acknowledgments

This research was supported by National Science Foundation Grant ATMS0129374. D. Leon processed the WCR radial velocities, and S. Haimov was responsible for the WCR data collection in IHOP. Figure 11 was provided by R. Damiani. This study greatly benefited from the review comments of A. Drake.

References Cited

Achtemeier, G. L. 1991. The use of insects as tracers for "clear-air" boundary-layer studies by Doppler radar. J. Atmos. Ocean. Tech. 8: 746–765.

Atlas, D. 1959. Radar studies of meteorological angel echoes. J. Atmos. Terrest. Phys. 15: 262–278.

Atlas, D., J. I. Metcalf, J. H. Richter, and E. E. Gossard. 1970. The birth of "CAT" and microscale turbulence. J. Atmos. Sci. 27: 903–913.

Campistron, B. 1975. Characteristic distributions of angel echoes in the lower atmosphere and their meteorological implications. Boundary-Layer Meteor. 9: 411–426.

Clothiaux, E. E., T. P. Ackerman, G. G. Mace, K. P. Moran, R. T. Marchand, M. A. Miller, and B. E. Martner. 2000. Objective determination of cloud heights and radar reflectivities using a combination of active remote sensors at the ARM CART sites. J. Appl. Meteor. 39: 645–665.

Dean, T. J., and V. A. Drake. 2002. Properties of biotic targets observed with an X-band radar profiler and the potential for bias in winds retrieved from Doppler weather radars. Proceedings of the 11th Australasian Remote Sensing and Photogrammetry Conference, Brisbane, Australia. 8–13 August 2002.

Drake, V. A. 1982. Insect in the sea-breeze front at Canberra: a radar study. Weather. 37: 134–143.

Drake, V. A. 1985. Solitary wave disturbances of the nocturnal boundary-layer revealed by radar observations of migrating insects. Boundary-Layer Meteor. 31: 269–286.

Drake, V. A., and R. A. Farrow. 1988. The influence of atmospheric structure and motions on insect migration. Annu. Rev. Entomol. 33: 183–210.

Drake, V. A., and R. A. Farrow. 1989. The aerial plankton and atmospheric convergence. Trends Ecol. Evol. 4: 381–385.

Geerts, B. and Q. Miao. 2005. A simple numerical model of the flight behavior of small insects in the atmospheric convective boundary layer. Environ. Entomol. 34: 361–368.

Glick P. A. 1960. Collecting insects by airplane, with special reference to the dispersal of the potato leafhopper. U.S. Department of Agriculture, Tech. Bull. 1222, 16 pp.

Greenbank, D. O., G. W. Schaefer, and R. C. Rainey. 1980. Spruce budworm (Lep. Tort.) moth flight and dispersal: new understanding from canopy observations, radar, and aircraft. Mem. Entomol. Soc. Can. 110: 1–49.

Gossard, E. E. 1990. Radar research on the atmospheric boundary layer, pp. 477–527. *In* D. Atlas (ed.), Radar in meteorology. American Meteorology Society, Boston, MA.

Hardy, K. R. 1968. CPS-9 radar investigations of clear-air convection, pp. 181–184. *In* Preprint volume, 13th Conference on Radar Meteorology. American Meteorology Society, Boston, MA. 7–13 July 1968.

Hardy, K. R., and H. Ottersten. 1969. Radar investigations of convective patterns in the clear atmosphere. J. Atmos. Sci. 26: 666–672.

Hardy, K. R., D. Atlas, and K. M. Glover. 1966. Multi-wavelength backscatter from the clear atmosphere. J. Geophys. Res. 71: 1537–1552.

Isard, S. A., and M. E. Irwin. 1993. A strategy for studying the long-distance aerial movement of insects. J. Agric. Entomol. 10: 283–297.

Isard, S.A., and S.H. Gage. 2001. Flow of life in the atmosphere: an airscape approach to understanding invasive organisms. Michigan State University Press, East Lansing, MI.

Isard, S. A., M. E. Irwin, and S. E. Hollinger. 1990. Vertical distribution of aphids (Homoptera:Aphididae) in the planetary boundary layer. Environ. Entom. 19: 1473–1484.

Johnson, C. G. 1957. The distribution of insects in the air and the empirical relation of density to height. J. Anim. Ecol. 26: 479–494.

Johnson, C. G. 1969. Migration and dispersal of insects by flight. Methuen, London, UK.

Knight, C. A., and L. J. Miller. 1998. Early radar echoes from small, warm cumulus: Bragg and hydrometeor scattering. J. Atmos. Sci. 55: 2974–2992.

Konrad, T. G. 1970. The dynamics of the convective process in clear air as seen by radar. J. Atmos. Sci. 27: 1138–1147.

LeMone, M. A. 1973. The structure and dynamics of horizontal roll vortices in the planetary boundary layer. J. Atmos. Sci. 30: 1077–1091.

LeMone, M. A., R. L. Grossman, F. Chen, K. Davis, and B. Geerts. 2003. The effects of surface heterogeneity on boundary-layer structure and energy fluxes from aircraft, pp. 44–48. *In* Preprint volume, symposium on observing and understanding the variability of water in weather and climate. American Meteorology Society, Boston, MA. 12–18 January 2003.

Leon, D. C., and G. Vali. 1998. Retrieval of three-dimensional particle velocities from airborne Doppler radar data. J. Atmos. Oceanic Tech. 15: 860–870.

Markowski, P. 2004. Multiple-Doppler radar observations of the structure and evolution of vortices in a convective boundary layer, p. 13.2. *In* Preprint volume, 22nd Conference on Local Severe Storms. American Meteorology Society, Boston, MA. 3–9 October 2004.

Mason, P. J. 1989. Large-eddy simulation of the convective atmospheric boundary layer. J. Atmos. Sci. 46: 1492–1516.

Miller, E. R., and R. B. Friesen. 1985. Standard output data products from the NCAR Research Aviation Facility. National Center for Atmospheric Research, Boulder, CO.

Pazmany, A., R. McIntosh, R. Kelly, and G. Vali. 1994. An airborne 95 GHz dual-polarized radar for cloud studies. IEEE Trans. Geosci. Remote Sensing. 32: 731–739.

Pedgley, D. E., D. R. Reynolds, J. R. Riley, and M. R. Tucker. 1982. Flying insects reveal small-scale wind systems. Weather. 37: 295–306.

Rainey, R. 1976. Flight behavior and features of the atmospheric environment, pp. 75–112. *In* R. C. Rainey (ed.), Insect flight. Royal Entomology Society, London, UK.

Reid, D. G., K. G. Wardhaugh, and J. Roffey. 1979. Radar studies of insect flight at Benalla, Victoria, in February 1974. CSIRO Australia Division of Entomology, Tech. Paper No. 16, 21 pp.

Reynolds, D. R. 1988. Twenty years of radar entomology. Antenna. 12: 44–49.

Richter, J. H., D. R. Jensen, V. R. Noonkester, J. B. Kreasky, and M. W. Stimmann. 1973. Remote radar sensing: atmospheric structure and insects. Science. 180: 1176–1178.

Riley, J. R. 1985. Radar cross section of insects. Proc. IEEE. 73: 228–232.

Riley, J. R. 1999. Radar returns for insects: implications for meteorological radars, pp. 390–392. *In* Preprint volume, 29th Conference on Radar Meteorology. American Meteorology Society, Boston, MA. 18–24 July 1999.

Russell, R. W., and J. W. Wilson. 1997. Radar-observed "fine lines" in the optically clear boundary layer. Reflectivity contributions from aerial plankton and its predators. Boundary-Layer Meteor. 82: 235–262.

Schaefer, G. W. 1976. Radar observations of insect flight, pp. 157–197. *In* R.C. Rainey (ed.), Insect flight. Royal Entomology Society, London, UK.

Stull, R. B. 1988. An introduction to boundary layer meteorology. Kluwer Academic, Dordrecht, The Netherlands.

Vaughn, C. R. 1985. Birds and insects as radar targets: a review. Proc. IEEE. 73: 205–227.

Weckwerth, T. M., J. W. Wilson, and R. M. Wakimoto. 1996. Thermodynamic variability within the convective boundary layer due to horizontal convective rolls. Mon. Wea. Rev. 124: 769–784.

Wilson, J. W., and W. E. Schreiber. 1986. Initiation of convective storms by radar-observed boundary-layer convergent lines. Mon. Wea. Rev. 114: 2516–2536.

Wilson, J. W., T. M. Weckwerth, J. Vivekanandan, R. M. Wakimoto, and R. W. Russell. 1994. Boundary-layer clear-air radar echoes: origin of echoes and accuracy of derived winds. J. Atmos. Ocean. Tech. 11: 1184–1206.

Received for publication 6 January 2004; accepted 12 January 2005.